# Numerical Investigation of Mixing Efficiency of Helical Ribbons

**J. de la Villéon**
Dept. of Chemical Engineering, Ecole Polytechnique, Montreal, Que., Canada, H3C 3A7
and
Elf Atochem, Centre d'Étude de Recherche et de Développement, 27470 Serquigny, France

**F. Bertrand and P. A. Tanguy**
URPEI-Paprican Chair, Dept. of Chemical Engineering, Ecole Polytechnique, Montreal, Que., Canada, H3C 3A7
Rhéotek Inc., Montreal, Que., Canada, H1M 3L8

**R. Labrie**
Dept. of Chemical Engineering, Ecole Polytechnique, Montreal, Que., Canada, H3C 3A7

**J. Bousquet**
Elf Aquitaine, CRES, 69630 Solaize, France

**D. Lebouvier**
Elf Atochem, Centre d'Étude de Recherche et de Développement, 27470 Serquigny, France

Helical ribbon impellers are often used for the mixing of viscous fluids because of their rather good homogenization potential. The questions that often arise concern the type of helical ribbon that performs the best in a given situation. Should one opt for a single helical ribbon or a double helical ribbon? What is the impact of a central screw on the overall mixing? Quite clearly, the answer to such questions is nontrivial since the quality of mixing achieved in a vessel depends on various parameters such as the geometry of the mixing equipment, the operating conditions, and the fluid rheology.

Viscous mixing with helical ribbons has been the subject of a number of investigations (Brito de la Fuente, 1992). Among those, Tanguy et al. (1992a) showed in a preliminary study that numerical modeling is a valuable asset for the prediction of mixing efficiency in such stirred vessels. Once the velocity field is known, one can resort to a wealth of mixing criteria the combination of which can provide some insight into the efficiency of the corresponding mixing device.

Mixing efficiency is often investigated qualitatively by computing the trajectories of a few clustered tracers and by studying their dispersion with time (Tanguy et al., 1992b, 1994). As these trajectories are the solution of the differential equation $dx/dt = u$, a fairly large amount of work has also focused on methods relying upon dynamical systems and chaos analysis (Ottino, 1989). For instance, several authors have based their investigations on the concept of *Poincaré sections* to detect *isolated islands* within which the flow is regular and the mixing is rather poor (Aref, 1984; Swanson and Ottino 1990; Muzzio et al., 1991; Kusch and Ottino, 1992; Niederkorn and Ottino, 1993; Jana et al., 1994; Harvey et al., 1996). The determination of the *length stretch* and the corresponding (maximum) *Lyapunov exponent*, is another way of estimating the chaotic behavior of a flow and consequently its potential to increase the stretching of a filament of tracers with time (Ottino, 1989).

The major difficulty with the above mixing criteria is to calculate with accuracy a trajectory for a long period of time, owing to the exponential growth of the numerical error (Souvaliotis et al., 1995). In particular, this represents quite a challenge for complicated three-dimensional (3-D) flows, as pointed out by the scarcity of numerical results found in such a case.

Another mixing criterion, which is related to the *length stretch* and the *Lyapunov exponent*, was suggested by Ottino (1989). Called *stretching efficiency*, it is not based on the computation of tracer trajectories, but rather on the value of the rate-of-strain tensor. It can be viewed as the local energy dissipated for the stretching of material elements. Bigio and Conner (1995) recently demonstrated that this measure of efficiency can be factored into two terms that they call the *line efficiency* and the *flow efficiency*. They respectively describe

Correspondence concerning this article should be addressed to P. A. Tanguy.

how close to the direction of maximum stretch the orientation of a line is and quantify the amount of energy which is transmitted to this same direction.

Finally, another efficiency coefficient based on the rate of strain and vorticity tensors was introduced by Manas-Zloczower (1993). Called the *dispersive mixing efficiency coefficient* (as opposed to the previous criteria which pertain to distributive mixing), it measures the relative importance of extensional effects over rotational effects in a flow, a large value indicating a better dispersion of a minor phase into a major phase. As mentioned by Huilgol (1975), this class of criteria based on the vorticity tensor is, however, of limited use owing to its lack of objectivity. This point will be discussed later.

The objective of this article is to study the mixing efficiency of an industrial reactor fitted up with three different helical ribbon impellers. To this end, criteria that we deem complementary will be used: *dispersion of tracers, length stretch* values and their associated *Lyapunov exponents*, and finally *dispersive mixing efficiency coefficients*. All these measures are based on flow simulations with finite-element software POLY3D from RheoTek Inc.

## Flow Simulation

The mixing vessel used for the study is cylindrical and has a dished bottom. With a diameter of 2.5 m and a volume of fluid of 8 $m^3$, its dimensions are typical of those encountered on polymer production lines. Three different agitators rotating at 5 rpm (Figure 1) will be tested: a single helical ribbon (HR), a double helical ribbon (DHR), and a double helical ribbon with a central screw (DHRS). The fluid considered is an industrial shear-thinning polymer the viscosity of which obeys a Carreau-A model (Bird et al., 1977).

The simulation of the motion in the tank is governed by momentum balance and continuity equations. Flow regime is laminar. The simulations are carried out with 3-D finite-element code POLY3D. Instead of generating one different mesh for every impeller type, it was decided to generate one single mesh representing the tank only and to model each impeller using a fictitious domain method called the virtual finite-element method (Bertrand et al., 1997). With this method, an impeller is approximated by a series of control points on which kinematic constraints are enforced via Lagrange multipliers. The mesh of the tank comprises 24,142 $P_1^+ - P_0$ linear elements (Bertrand et al., 1992) resulting in 152,378 velocity equations. Moreover, to ease the imposition of the boundary conditions, it was decided to consider the viewpoint of an observer located on the moving impeller. In such a (Lagrangian) frame of reference, the boundary conditions are as follows:

- A no-slip condition on the (nonmoving) impeller;
- The rotational speed on the vessel walls; and
- Free surface conditions (the surface is assumed to be flat).

Considering that the Reynolds number is about 0.5, the free surface assumption is realistic. The simulations were carried out on an IBM RISC 6000/590 workstation. Each simulation required about 150 MB of memory and a few hours of CPU time. This is comparable to the time it took to perform the computations inherent to the tests below.

## Flow Analysis

### *Computation of trajectories*

The quantitative mixing criteria used in this work are all based upon a known velocity field and, except for one case, they require the computation of tracer trajectories. These are obtained by integrating the velocity over time using a variable time-stepping fourth-order Runge-Kutta scheme for

$$x(t) = x(0) + \int_0^t v(x(t'))dt'. \qquad (1)$$

As mentioned by Souvaliotis et al. (1995), when combined with a sufficiently refined mesh, adaptive high-order integration methods can generate relatively accurate trajectories the overall error of which is controlled by the discretization error, that is, the coarseness of the finite-element mesh used. Of course, when the flow is chaotic, the computational time may become prohibitive owing to the very small time steps that come into play. Fortunately, these same researchers observed that, even in the case of a coarse mesh and some reasonable time step, the total error behaves as a material line that deforms and orients in such a way that the overall mixing patterns can be reproduced qualitatively. They, however, pointed out that, if the main characteristics of a trajectory can be predicted, its length can be substantially different. Fi-

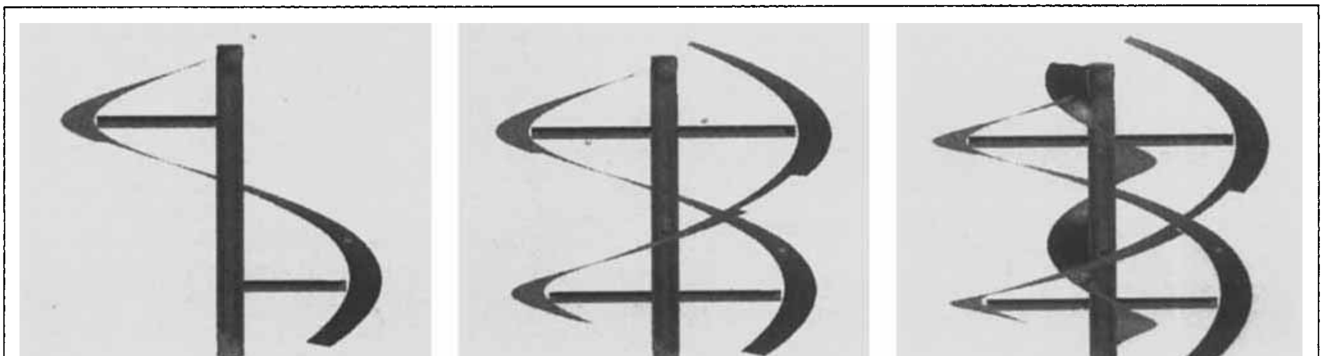

**Figure 1. Helical ribbon impellers.**

nally, despite these theoretical limitations, it is worthwhile noting that good quantitative agreement between numerical and experimental circulation times have been obtained in the case of an helical ribbon screw impeller system (Tanguy et al., 1992a)..

### *Dispersion of clustered tracers*

We adapted Danckwerts' *intensity of segregation* measure (Danckwerts, 1952) to study the *dipsersion of clustered tracers* in the tank and thus get an idea of the overall dynamics of mixing. More precisely, the concentration (number fraction) of tracers in each finite element $i$, $C_i$, is calculated at each time step as

$$C_i = \frac{N_i V}{N V_i}, \tag{2}$$

where $N_i$ denotes the number of tracers in element $i$, $V_i$, the volume of this element, and $N$ and $V$ denote similar quantities for the whole domain. The standard deviation of the concentration (also called coefficient of variation) in the tank is then defined as

$$s = \frac{\sqrt{\dfrac{\sum_{i=1}^{M}(C_i - \bar{C})^2}{M-1}}}{\bar{C}}, \tag{3}$$

where $M$ is the number of elements, and $\bar{C}$ the mean value of the concentration. Take also note that $s$ is scaled so that it takes on values between 0 (optimal dispersion) and 1 (complete segregation). Consequently, in an ideal system, it is expected to go down to 0 very quickly in time.

The results obtained for all three impellers are presented in Figure 2. 5,000 tracers were launched in each case. It can be readily noted that the time at which the curves level off is about 170 s for the HR impeller and about 130 s for the DHR and DHRS impellers. These numbers can be interpreted as *mixing times* insofar as they indicate when the tracer concentrations stabilize. However, for reasons mentioned above concerning the error in the length of the trajectories, they should be used at the most as relative indicators. This being said, on the basis of this test, the use of a double helical ribbon leads to a drop in the mixing time and the addition of a central screw makes no improvements. Such a phenomenon was also observed both numerically and experimentally by Tanguy et al. (1992b); the presence of a central screw, which adds to the power draw, does not enhance axial pumping sufficiently to generate a significant reduction of the mixing time. One must also keep in mind that changing the initial position of the drop may affect the results. In particular, if tracers are launched in the middle of a dead zone or an isolated island, then a stabilization in the shape of the curve should by no means suggest a mixing time; mixing time makes sense only in the case of a well-mixed system. Moreover, the relatively modest amount of tracers (with respect to the number of finite elements) launched in the tank is responsible for the occurrence of wiggles on the curves, especially at early time steps. This was confirmed by other tests attempted with more tracers that also revealed no significant changes in the mixing times. Finally, the fact that the final values of $s$ satisfy $s_{HR} < s_{HRS} < s_{DHRS}$, which may look suspicious at first sight, is owing to the use of a fictitious domain method. A relative number of finite elements contain kinematic conditions (to account for the impeller), so that they cannot be traversed by tracers. Therefore, the standard deviations are overestimated. The above property is a direct consequence of the fact that there are more such elements for the DHRS than for the HRS, and more for the HRS than for the HR.

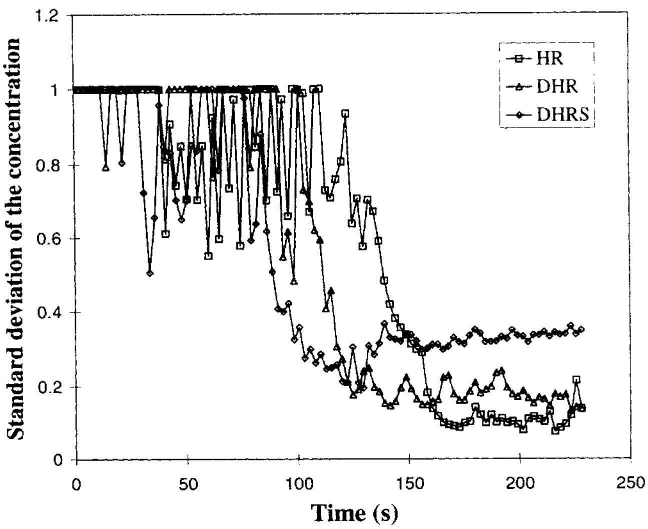


**Figure 2. Dispersion of clustered tracers.**

### *Dispersion of tracers initially located in the lower half of the tank*

The previous test gives an idea of the quality of dispersion in all three dimensions. One way to assess the pumping potential of a mixing system consists of tracking down tracers initially located in the lower half of the tank and monitoring the percentage $R$ of these tracers that are located there.

Initially, $R = 1$ since all the tracers are located in the lower half of the tank. The value of $R$ then decreases with time due to tracer migration, and if there are no segregated regions, should ideally converge to 0.5 when the same number of tracers are found in the lower and upper halves of the tank. By analogy with the previous test, one can then define the mixing time as the time it takes for the curve $R$ vs. time to level off to some plateau (ideally to 0.5).

This method was applied to a group of 1,500 tracers. As can be noted in Figure 3, the number of tracers in the lower half of the tank decreases faster with time when a double helical ribbon is used. In all three cases, the rates end up oscillating between 0.5 and 0.65, which indicates a rather good distribution. A look at the final tracer distribution (not shown here) confirms this fact. Once again, the central screw does not seem to play a significant role, which is rather surprising since its main asset is precisely to enhance pumping. From a quantitative point of view and keeping in mind the above comments concerning the error in the length of trajectories, it can be seen that the mixing times for the single and double

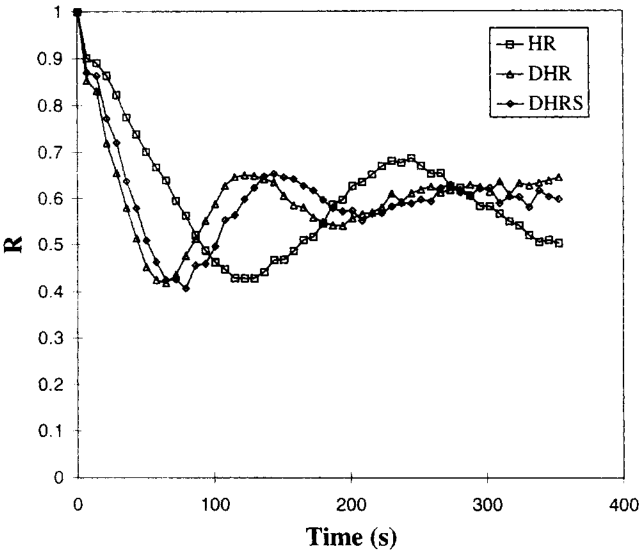


**Figure 3. Dispersion of tracers launched in the lower half of the tank.**

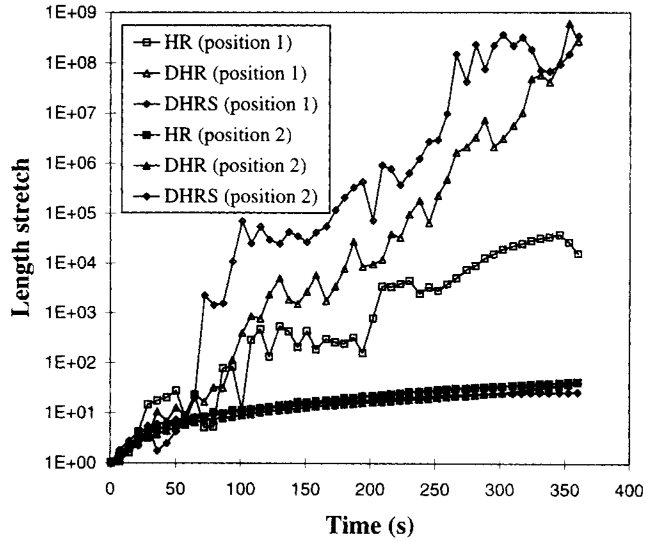


**Figure 4. Length strength values.**

helical ribbon impellers are more than 350 s (the corresponding curve has not stabilized yet) and about 250 s, respectively. It appears that these values are much larger (by a factor of about two) than those obtained with the previous test. One must, however, realize that they reflect only the vertical motion (along the $z$ axis) within the tank and, contrary to the previous test, do not take into account in-plane mixing, that is, tracer distribution in the $x$- and $y$- directions. As a result, it should come as no surprise that the mixing times obtained with both tests differ.

### *Length stretch and Lyapunov exponent*

It is well known that chaotic flow leads to efficient mixing, that is, to stretching and folding of material lines and surfaces (Aref, 1984). Consequently, the stirring potential of an impeller is related to the amount of stretching it can generate anywhere in the reactor, which can be quantified by what is referred to as the *length stretch*

$$\lambda = \lim_{\|dX\| \to 0} \frac{\|dx\|}{\|dX\|}, \tag{4}$$

where $dX$ represents an infinitesimal line in its initial (reference) state and $dx$ its deformation at time $t > 0$ when subject to a velocity $v$. As shown by Franjione and Ottino (1987), the accurate tracking of material lines can be very costly. To alleviate this problem, one can resort to a technique put forward by Benettin et al. (1976) and further explained by Wolf et al. (1984). In short, it consists of computing the length stretch value for a material line as the product of length stretch values for companion lines defined over time intervals within each of which the length growth is not too large. This avoids the need, during the course of the calculations, to inject extra discretization points to control tracking accuracy (Muzzio et al., 1991).

In a chaotic flow, a material line grows exponentially with time and the length stretch calculated by the above technique is related to the maximum *Lyapunov exponent* $\sigma$ through the relation

$$\sigma = \lim_{t \to \infty} \frac{\log \lambda}{t} \tag{5}$$

or

$$\lambda \approx e^{\sigma t} \tag{6}$$

when $t$ is large. Moreover, as observed by Benettin et al. (1976), the value of $\sigma$ does not depend on $dX$ as long as $\|dX\|$ is sufficiently small. In this work, the computation of Lyapunov exponents using 100 different orientations of the vector $dX$ confirmed this observation.

Length stretch values were computed for all three impellers starting with two different positions for initial line $dX$, that is, in the upper part of the tank and at the bottom of the tank, respectively. Figure 4 contains a graph showing the evolution of $\lambda$ with time from which a value for $\sigma$ can be deduced using relation 6.

For position 1, that is, in the upper part of the tank, one readily sees that the length stretch grows exponentially. In fact, it follows from Table 1 that a 60% increase in $\sigma$ is obtained when switching from the single to the double helical impeller, while the addition of a central screw to the latter only boosts $\sigma$ by a mere 20%, a result which complies with the previous criteria.

A completely different trend can be noted for position 2 at the bottom of the tank. Contrary to the other position, the length stretch curves rise very poorly. One can indeed note that in each case the Lyapunov exponent asymptotically tends

**Table 1. Values of the Lyapunov Exponent for Position 1**

| Impeller | $\sigma$ |
|---|---|
| HR | 0.033 |
| DHR | 0.052 |
| DHRS | 0.062 |

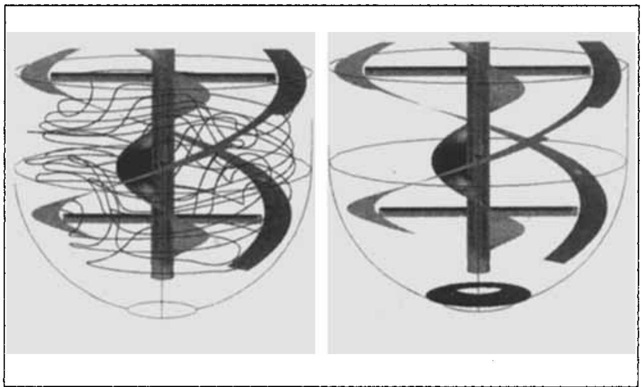

**Figure 5. Tracer trajectories for positions 1 and 2.**

towards zero, which means that the flow is regular (nonchaotic) in this region. As pointed out in Figure 5, which displays the tracer trajectory for each position, the bottom of the tank is indeed a segregated region with rather poor mixing. The calculation of Lyapunov exponents, therefore, provides a way of assessing local aspects of mixing by quantifying the stretching capability of a flow, as well as discerning regular and chaotic regions in an industrial reactor.

The *stretching efficiency* (Ottino, 1989) is another tool that can be used to gauge the quality of mixing in a reactor. Calculations of this measure confirmed the previous findings, but did not shed any more light, which is not surprising at all since it is related to the length stretch and the Lyapunov exponent. For this reason, these results are not presented here.

### *Dispersive mixing efficiency*

Finally, the *dispersive mixing efficiency coefficient* of Manas-Zloczower (1993) was computed at various locations in the reactor. Based on the local value of the rate-of-strain tensor, it measures the relative importance of extensional effects over rotational effects in a flow. What provided the impetus for the development of this criterion was the fact that, in the laminar regime, elongational flows of inelastic fluids are generally more effective than simple shear flows for breaking up and dispersing a minor phase into a major phase. A physical explanation is that, in shear flows, macromolecules are rotating in the shear plane so that stretching is relatively poor, whereas, in elongational flows, the polymeric chains are aligned in the flow direction so that they can stretch more efficiently (Agassant et al., 1991). Consequently, they can disperse more quickly.

The dispersive mixing efficiency coefficient is defined as follows:

$$\alpha = \frac{\| \dot{\gamma} \|}{\| \dot{\gamma} \| + \| \omega \|} \quad (7)$$

where $\omega = \frac{1}{2}[\nabla v - (\nabla v)^T]$ is the vorticity tensor. As mentioned in the introduction, this class of criteria based on the vorticity tensor is of limited use owing to its lack of objectivity. We note, however, that only one frame of reference is considered in this work. We nevertheless recognize that a frame invariant criterion, such as the one proposed by Astarita (1979) which involves the objective rate-of-rotation tensor introduced by Drouot and Lucius (1976), would be more appropriate to classify flow fields from different frames of reference.

Nodal values of $\alpha$ were computed for all three impellers. Figure 6 displays a fringe plot of $\alpha$ on a cross-section plane for values satisfying $\alpha \leq 0.4$. Every gray shade represents a 0.1 wide variation for $\alpha$, a darker tone denoting a smaller value. One readily sees that the size of the shaded area is much larger for the single helical ribbon than for the double helical ribbon impellers, revealing a more effective dispersion in the latter case. In fact, the symmetric pattern in the case of the DHR impeller (nearly symmetric in the case of the DHRS impeller) clearly shows the enhancement provided by the second ribbon. One may also note the presence of a dark region underneath the impeller shaft, at the bottom of the tank, which signifies a rotation-dominated flow in this area. This fact is corroborated in Figure 5.

An in-depth analysis shows that the volumetric distributions of $\alpha$ (Figure 7) are rather broad. In particular, the curve corresponding to the HR impeller appears as shifted leftward with respect to the other two curves, which indicates a less important elongational effect. More precisely, the mean value of $\alpha$, denoted by $\overline{\alpha}$, is significantly larger in the case of the double helical ribbon impellers (Table 2). On the basis of this test, one would then expect dispersive mixing to be more efficient with this impeller type.

**Figure 6. Fringe plot on a cross-section plane for $\alpha \leq 0.4$.**

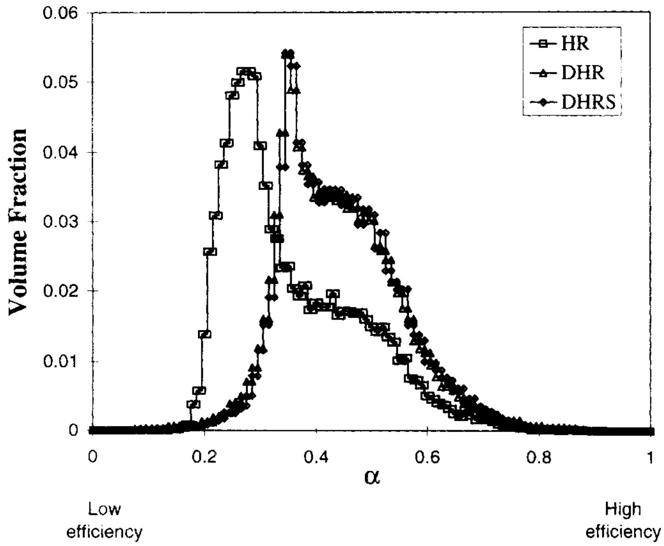


**Figure 7. Volumetric distribution of parameter $\alpha$.**

**Table 2. Values of $\bar{\alpha}$**

| Impeller | $\bar{\alpha}$ | Standard Deviation |
|---|---|---|
| HR | 0.357 | 0.126 |
| DHR | 0.441 | 0.114 |
| DHRS | 0.446 | 0.115 |

## Conclusion

In this article, different mixing criteria were used to study the stirring efficiency of three helical ribbon impellers mounted in an industrial batch tank. These criteria all led to the same conclusion that, at least for the shear-thinning polymer considered in this work, the double helical ribbon impellers are more efficient and that adding a central screw does not enhance mixing significantly. It must be emphasized that only parameters related to the mechanisms of mixing were studied here. A more thorough investigation should also include an analysis of the power draw and the energy needed for mixing, as these are key factors in the design of stirred tanks.

## Acknowledgments

We would like to thank the referees who brought to our attention the references related to objective rate-of-rotation tensors.

## Literature Cited


Agassant, J. A., P. Avenas, J. Ph. Sergent, and P. Carreau, *Polymer Processing, Principles and Modeling*, Hanser Publishers, Munich (1991).

Aref, H., "Stirring by Chaotic Advection," *J. Fluid Mech.*, **143**, 1 (1984).

Astarita, G., "Objective and Generally Applicable Criteria for Flow Classification," *J. Non-Newt. Fluid Mech.*, **6**, 69 (1979).

Benettin, G., L. Galgani, and J.-M. Strelcyn, "Kolmogorov Entropy and Numerical Experiments," *Phys. Rev.*, **A14**, 2338 (1976).

Bertrand, F., M. Gadbois, and P. A. Tanguy, "Tetrahedral Elements for Fluid Flow Problems," *Int. J. Num. Meth. Eng.*, **33**, 1251 (1992).

Bertrand, F., P. A. Tanguy, and F. Thibault, "A Three-Dimensional Fictitious Domain Method For Incompressible Fluid Flow Problems," *Int. J. Num. Meth. Fluids*, **25**, 719 (1997).

Bigio, D. I., and J. H. Conner, "Principle Directions as a Basis for the Evaluation of Mixing," *Poly. Eng. and Sci.*, **35**, 1527 (1995).

Bird, R. B., R. C. Armstrong and O. Hassager, *Dynamics of Polymeric Liquids*, Wiley, New York (1977).

Brito de la Fuente, E., "Mixing of Rheological Complex Fluids with Helical Ribbon and Helical Screw Ribbon Impellers," PhD Thesis, Laval University, Quebec City, Que (1992).

Danckwerts, P. V., "The Definition and Measurement of Some Characteristic Mixtures," *Appl. Sci. Res.*, **A3**, 279 (1952).

Drouot, R., and M. Lucius, "Approximation du Second Ordre de la Loi de Comportement des Fluides Simples. Lois Classiques déduites de l'introduction d'un Nouveau Tenseur Objectif," *Arch. Mech. Stasow.*, **28**, 189 (1976).

Franjione, J. G., and J. M. Ottino, "Feasibility of Numerical Tracking of Material Lines and Surfaces in Chaotic Flows," *Phys. Fluids*, **30**, 3641 (1987).

Harvey, A. D., D. H. West, D. Kronholm, M. Frank, and N. Tufillaro, "Computational Analysis of Chaotic Laminar Mixing in Stirred Tanks with Multiple Impellers," AIChE Meeting, Chicago (1996).

Huilgol, R. R., "On the Concept of the Deborah Number," *Trans. Soc. Rheol.*, **19**, 297 (1975).

Jana, S. J., G. Metcalfe, and J. M. Ottino, "Experimental and Computational Studies of Mixing in Complex Stokes Flows: the Vortex Mixing Flow and Multicellular Cavity Flows," *J. Fluid Mech.*, **269**, 199 (1994).

Kusch, H. A., and J. M. Ottino, "Experiments on Mixing in Continuous Chaotic Flows," *J. Fluid Mech.*, **236**, 319 (1992).

Manas-Zloczower, I., "Studies of Mixing Efficiency in Batch and Continuous Mixers," *Rubber Chem. Tech.*, **67**, 504 (1993).

Muzzio, F. J., P. D. Swanson, and J. M. Ottino, "The Statistics of Stretching and Stirring in Chaotic Flows," *Phys. Fluids A.*, **3**, 822 (1991).

Niederkorn, T. C., and J. M. Ottino, "Mixing of Viscoelastic Fluid in a Time-Periodic Flow," *J. Fluid Mech.*, **256**, 243 (1993).

Ottino, J. M., *The Kinematics of Mixing: Stretching, Chaos, and Transport*, Cambridge University Press, Cambridge, U.K. (1989).

Souvaliotis, A., S. C. Jana, and J. M. Ottino, "Potentialities and Limitations of Mixing Simulations," *AIChE J.*, **41**, 1605 (1995).

Swanson, P. D., and J. M. Ottino, "A Comparative Computational and Experimental Study of Chaotic Mixing in Viscous Fluids," *J. Fluid Mech.*, **213**, 227 (1990).

Tanguy, P. A., R. Lacroix, F. Bertrand, L. Choplin, and E. Brito-De La Fuente, "Finite Element Analysis of Viscous Mixing With an HRS Impeller," *AIChE J.*, **38**, 939 (1992a).

Tanguy, P. A., R. Lacroix, F. Bertrand, L. Choplin, and E. Brito-De La Fuente, "Mixing of Non-Newtonian Viscous Fluids with Helical Impellers: Experimental and 3D Numerical Studies," *Process Mixing—Chemical and Biochemical Applications*, AIChE Symp. Ser., No. 286, G. Tatterson and R. Calabrese, eds., p. 33 (1992b).

Tanguy, P. A., F. Bertrand, and E. Brito de la Fuente, "Mixing of Viscoplastic Fluids With Anchor Impellers," *Proc. Euro. Conf. on Mixing*, Cambridge, U.K. (1994).

Wolf, A., J. B. Swift, H. L. Swinney, and J. A. Vastano, "Determining Lyapunov Exponents from a Time Series," *Physica D*, **16**, 285 (1984).


*Manuscript received June 24, 1997, and revision received Jan. 21, 1998.*